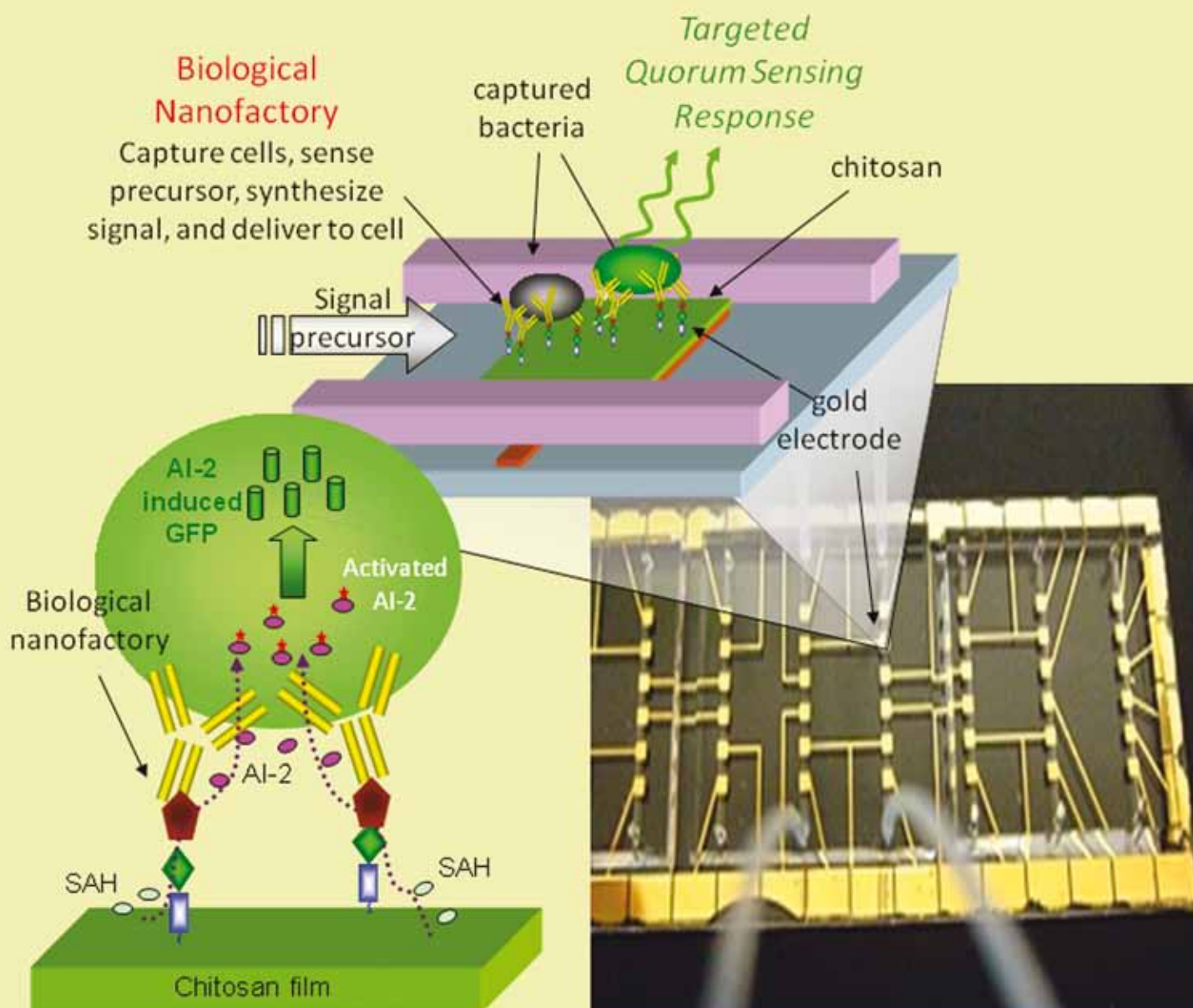


# Lab on a Chip

Micro- & nano- fluidic research for chemistry, physics, biology, & bioengineering

www.rsc.org/loc

Volume 10 | Number 9 | 7 May 2010 | Pages 1097–1212



ISSN 1473-0197

RSC Publishing

Bentley  
Biological nanofactories

Burns  
Rapid 2D arraying

Ozcan  
Lensless imaging

Retterer  
Nanoporous bioreactors

# Biological nanofactories facilitate spatially selective capture and manipulation of quorum sensing bacteria in a bioMEMS device

Rohan Fernandes,<sup>†ab</sup> Xiaolong Luo,<sup>†ab</sup> Chen-Yu Tsao,<sup>ab</sup> Gregory F. Payne,<sup>b</sup> Reza Ghodssi,<sup>cd</sup> Gary W. Rubloff<sup>ede</sup> and William E. Bentley<sup>\*ab</sup>

Received 22nd December 2009, Accepted 25th January 2010

First published as an Advance Article on the web 16th February 2010

DOI: 10.1039/b926846d

The emergence of bacteria that evade antibiotics has accelerated research on alternative approaches that do not target cell viability. One such approach targets cell–cell communication networks mediated by small molecule signaling. In this report, we assemble biological nanofactories within a bioMEMS device to capture and manipulate the behavior of quorum sensing (QS) bacteria as a step toward modifying small molecule signaling. Biological nanofactories are bio-inspired nanoscale constructs which can include modules with different functionalities, such as cell targeting, molecular sensing, product synthesis, and ultimately self-destruction. The biological nanofactories reported here consist of targeting, sensing, synthesis and, importantly, assembly modules. A bacteria-specific antibody constitutes the targeting module while a genetically engineered fusion protein contains the sensing, synthesis and assembly modules. The nanofactories are assembled on chitosan electrodeposited within a microchannel of the bioMEMS device; they capture QS bacteria in a spatially selective manner and locally synthesize and deliver the “universal” small signaling molecule autoinducer-2 (AI-2) at the captured cell surface. The nanofactory based AI-2 delivery is demonstrated to alter the progression of the native AI-2 based QS response of the captured bacteria. Prospects are envisioned for utilizing our technique as a test-bed for understanding the AI-2 based QS response of bacteria as a means for developing the next generation of antimicrobials.

## Introduction

Small molecule signaling is widely utilized in nature to control cellular function.<sup>1–3</sup> In bacteria, small molecule signaling has been shown to affect bioluminescence,<sup>4,5</sup> virulence,<sup>6,7</sup> biofilm formation<sup>8,9</sup> and other diverse phenotypes. Bacteria produce, secrete, sense and transduce small signaling molecules called autoinducers, in a process termed quorum sensing (QS)<sup>10</sup> which has been implicated in intra- and inter-species, as well as inter-kingdom communication.<sup>11</sup> With the emergence of antibiotic resistant bacteria that pose a serious risk to human health, methods that modulate or interrupt bacterial communication are being increasingly investigated.<sup>12,13</sup> These methods do not affect bacterial viability and therefore exert less selective pressure on them to develop resistance.<sup>14</sup>

We present a technique that utilizes biological nanofactories and electrodeposited chitosan to spatially capture and alter the response of QS bacteria within a bioMEMS device. BioMEMS

devices have been widely used for biological analysis as they provide benefits, including small device sizes, low reagent volumes, and the possibility for parallel processing.<sup>15–21</sup> They also provide a useful platform to study and manipulate QS based phenomena, such as biofilm formation, in controlled environments that can mimic those observed in native systems. Despite their utility, bioMEMS devices remain relatively underutilized in studying QS based phenomena.

Biological nanofactories<sup>22,23</sup> are bio-inspired nanoscale factories that are comprised of multiple modules, each performing a particular function including (1) specifically targeting cells, (2) sensing and transporting raw materials present in their vicinity, (3) converting the raw materials to useful molecules, (4) transporting them back to the cell surface and (5) self-destructing upon completion of this sequence. In our recent report,<sup>22</sup> we further demonstrated a module for assembly of the nanofactory itself. In that case it was a nanofactory consisting of four modules spatially aligned for efficient function: targeting, sensing, synthesis and an assembly module not originally contemplated<sup>23</sup> (Scheme 1a). The targeting module consisted of a bacteria targeting antibody. The components of fusion protein (*His*)<sub>6</sub>-Protein *G*-LuxS-Pfs-(Tyr)<sub>5</sub> (HGLPT)<sup>22</sup> constituted the sensing, synthesis and assembly modules. This construct is the same as in the current report. The enzyme *S*-adenosylhomocysteine nucleosidase (Pfs) purified from *Escherichia coli* is the sensing module that senses substrate *S*-adenosylhomocysteine (SAH) in its vicinity. Pfs and *S*-ribosylhomocysteinase (LuxS), also purified from *E. coli*, constitute the synthesis module that converts SAH into signaling autoinducer-2 (AI-2), a “universal”

<sup>a</sup>Fischell Department of Bioengineering, University of Maryland, College Park, MD, 20742, USA. E-mail: bentley@umd.edu; Fax: +1 301 405 9973; Tel: +1 301 405 4321

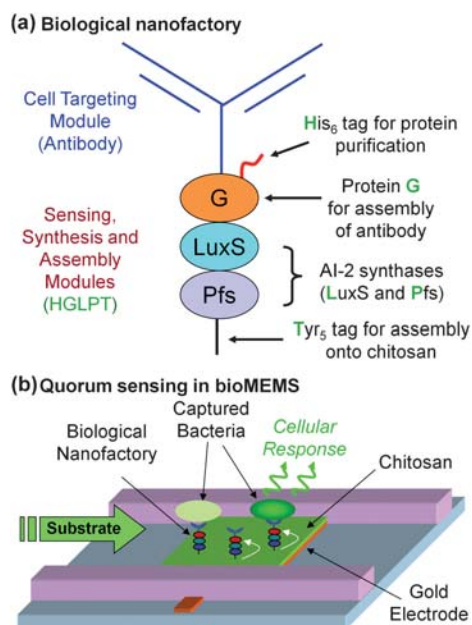
<sup>b</sup>Center for Biosystems Research, University of Maryland Biotechnology Institute (UMBI), College Park, MD, 20742, USA

<sup>c</sup>Department of Electrical and Computer Engineering, University of Maryland, College Park, MD, 20742, USA

<sup>d</sup>Institute for Systems Research (ISR), University of Maryland, College Park, MD, 20742, USA

<sup>e</sup>Department of Materials Science and Engineering, University of Maryland, College Park, MD, 20742, USA

<sup>†</sup> The first two authors contributed equally.



**Scheme 1** Assembly and manipulation of quorum sensing (QS) bacteria in a bioMEMS device *via* biological nanofactories. (a) Components of a biological nanofactory: cell targeting module (antibody); sensing, synthesis and assembly modules (HGLPT nano-construct). (b) The nanofactories are spatially assembled onto chitosan electrodeposited within the device; they capture targeted bacteria and manipulate their QS response.

signaling molecule observed in over 70 bacterial species.<sup>11,14</sup> The assembly module consists of protein G and the C-terminal pentatyrosine tag ((Tyr)<sub>5</sub>) of HGLPT. Protein G,<sup>24,25</sup> from group C and G *Streptococcus*, facilitates binding of fusion protein HGLPT to the targeting antibody while the pentatyrosine tag, used here for the first time, facilitates covalent attachment of the nanofactory to electrodeposited chitosan.<sup>26–29</sup>

Chitosan is an amine-group containing biopolymer with pH-dependent solubility.<sup>30,31</sup> When an electric current is imposed between two electrodes in a solution containing chitosan, it electrodeposits from solution onto the negatively charged electrode on account of a high pH generated in the vicinity of the negative electrode.<sup>32–35</sup> The overall scheme for assembly and manipulation of QS bacteria in a bioMEMS device (Scheme 1b) involves (1) fabrication and packaging of the device with electrodeposition of chitosan on the negative electrode (working electrode) within a microchannel, (2) assembly of the biological nanofactories *i.e.* spatially selective assembly of HGLPT and the targeting antibody on the working electrode, (3) capture of targeted QS bacteria (*E. coli*) by nanofactories, and (4) manipulation of the bacterial response within the device *via* nanofactory-facilitated localized synthesis and delivery of AI-2.

## Materials and methods

### Chemicals

Chitosan (medium molecular weight, average molecular weight 300 000 g mol<sup>-1</sup>), tyrosinase (from mushroom), phosphate buffered saline tablets (10 mM phosphate buffer, 2.7 mM KCl

and 137 mM NaCl, pH 7.4), albumin from bovine serum (BSA), *S*-(5'-deoxyadenosin-5')-L-homocysteine (SAH), 5,5'-dithiobis-(2-nitrobenzoic acid) (DTNB) and isopropyl β-D-1-thiogalactopyranoside (IPTG) were purchased from Sigma Aldrich. Ampicillin sodium salt, kanamycin, Tris, dibasic sodium phosphate (Na<sub>2</sub>HPO<sub>4</sub>·7H<sub>2</sub>O), monobasic sodium phosphate (NaH<sub>2</sub>PO<sub>4</sub>·H<sub>2</sub>O), sodium acetate trihydrate (CH<sub>3</sub>COONa·3H<sub>2</sub>O), sodium hydroxide (NaOH) and hydrochloric acid (HCl) were purchased from Fisher Scientific. Alexa Fluor 568 (excitation wavelength peak 555 nm and emission wavelength peak 565 nm) protein labeling kit was purchased from Invitrogen and blotter grade non-fat dry milk was purchased from Bio-Rad.

### Antibodies

Rabbit anti *E. coli* was purchased from AbD Serotec. Alexa Fluor 568 labeling of the antibody was performed as per the manufacturer's specification (www.invitrogen.com).

### Bacterial strains and growth conditions

The bacterial strains used in this study were *E. coli* BL21 carrying plasmid pGFP (IPTG inducible GFP)<sup>36</sup> and *E. coli* W3110 carrying plasmids pCT5 and pETGFP (AI-2 inducible GFP).<sup>37</sup> Both strains were grown in Luria-Bertani (LB) medium (Sigma Aldrich) at 37 °C with vigorous shaking (250 rpm). The LB medium used for bacterial growth contained 5 g L<sup>-1</sup> of yeast extract, 10 g L<sup>-1</sup> of Bacto Tryptone and 10 g L<sup>-1</sup> NaCl. Antibiotic concentrations used for the different strains were 50 μg mL<sup>-1</sup> ampicillin for *E. coli* BL21 (with plasmid pGFP) and 20 μg mL<sup>-1</sup> ampicillin and 50 μg mL<sup>-1</sup> kanamycin for *E. coli* W3110 (with plasmids pCT5 and pETGFP).

### BioMEMS device fabrication and packaging

The bioMEMS device (Fig. 1) was fabricated and packaged based on previous reports.<sup>29,38</sup> Briefly, the device consisted of

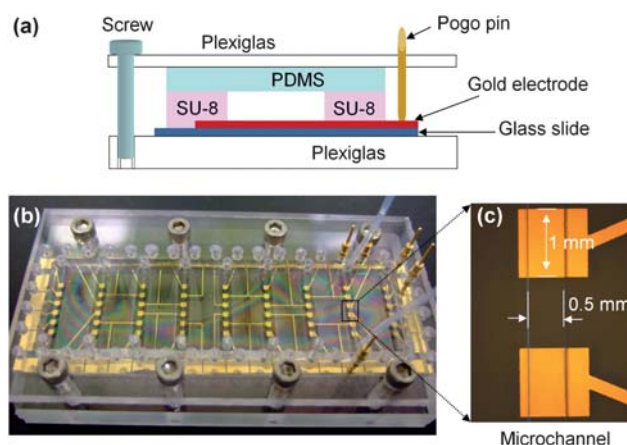


**Fig. 1** Perspectives of the bioMEMS device. (a) Cross-sectional schematic of the packaged bioMEMS device. The microchannel is defined by SU-8 structures on a glass slide containing patterned gold electrodes, packaged with PDMS and sandwiched between two Plexiglas plates. (b) The bioMEMS device contains nine microchannels; each channel containing six patterned gold electrodes. (c) Magnified view of a microchannel showing the negative (working) and positive electrodes.

9 microchannels evenly distributed on a glass slide (1" × 3") with six gold electrodes underneath each channel. A Cr adhesion layer (100 Å) and then a gold layer (2000 Å) were evaporated onto a 1" × 3" glass slide. Rectangular electrodes (1 mm × 1 mm) and electric contacts (2 mm × 2 mm around the edge of the glass slide) were patterned with photolithography. SU8-50 was patterned on the top of the substrate and electrode surfaces to form microchannels of 19 mm long, 150 μm high and 500 μm wide. This created an in-channel electrode area of 0.5 mm<sup>2</sup> and a channel volume of 0.075 μL above each electrode. The microchannels were then sealed with a 2 mm thick PDMS layer and the microchannel-PDMS complex was sandwiched between two Plexiglas plates. Pogo pins (mounting hole diameter 0.060") were inserted as electric connections and held with friction through holes (0.064" id) drilled on the top Plexiglas plate. Microbore PTFE tubing (0.022" id × 0.042" od) was connected to microchannels through the holes drilled on the top (0.064" id) Plexiglas and the holes punched through PDMS (by a Harris Uni-core punch, 1.0 mm).

### Chitosan preparation and electrodeposition

A 0.5% chitosan solution was prepared by adding chitosan flakes to de-ionized water that was stirred and maintained at pH ≈ 2 (by dropwise addition of HCl). After dissolution, the pH was raised to pH ≈ 5 by the dropwise addition of 1 M NaOH. De-ionized water was then added to adjust the final concentration. The resulting chitosan solution was filtered and stored at 4 °C. To electrodeposit chitosan, the microchannels were first prepared by rinsing with de-ionized water for at least 10 minutes. The microchannels were filled with chitosan solution, and an electrical signal of 3 A m<sup>-2</sup> was applied for 2 minutes to electrodeposit chitosan onto the negatively biased electrode (working electrode).<sup>29,35</sup> Immediately after the electrodeposition, the microchannels were gently rinsed with PBS to remove unbound chitosan.

### Spatially selective assembly of the biological nanofactories

Unless specified, PBS rinsing between two experimental steps to remove unbound molecules or cells was performed for 30 minutes at a flow rate of 5 μL min<sup>-1</sup>. After the electrodeposition of chitosan as described above, a blocking solution (5% non-fat milk in PBS) was introduced into the microchannel at a flow rate of 1 μL min<sup>-1</sup> for 2 hours to prevent non-specific adsorption of proteins onto the channel surfaces. After PBS rinsing, HGLPT which was purified as described in the literature<sup>22</sup> was attached onto the chitosan scaffold by introducing a solution containing 1 μM HGLPT and 50 U mL<sup>-1</sup> tyrosinase into the channel at a flow rate of 1 μL min<sup>-1</sup> for 1 hour. After PBS rinsing, 1 μM Alexa Fluor 568 labeled anti *E. coli* and 10 μM BSA were introduced at a flow rate of 1 μL min<sup>-1</sup> for 1 hour. The channel was once again rinsed with PBS. The fluorescence of the working electrode, reference electrode and channel background was observed under a fluorescence microscope (Carl Zeiss 310) and a UV source (Zeiss HBO 100) using a TRITC filter (Chroma, 545 nm/610 nm). Photographs were taken under a Zeiss 310 optical microscope with a digital camera (Carl Zeiss AxioCam MRc5) using 0.5–2 second exposure. As a control, all the above steps

were performed in another channel except the step involving the introduction of HGLPT and tyrosinase into the channel.

### Spatially selective capture of QS bacteria

*E. coli* BL21 carrying plasmid pGFP was cultured as described above. When the  $od_{600}$  of the cells was between 0.4 and 0.6, the cells were induced with 1 mM IPTG to overexpress GFP and the cells were incubated at 37 °C and 250 rpm for another 6 hours. The resultant fluorescent cells were collected by centrifuging at 10 000 × *g* for 5 minutes, resuspended in PBS containing 5% BSA and the  $od_{600}$  of the cells was adjusted to 0.4. Biological nanofactories (with the non-fluorescent antibody) were assembled as described earlier and the fluorescent cells were introduced into the channel at 1 μL min<sup>-1</sup> for 1 hour before the channel was rinsed with PBS. The fluorescence of the working electrode and channel background was observed under the fluorescence microscope using a Sapphire UV GFP filter (Chroma, 495 nm/510 nm). Photographs were taken with the digital camera using 2 second exposure. All the above steps were performed in the control channel except for the introduction of the nanofactories.

### Synthesis of *in vitro* AI-2 by the biological nanofactories at the surface of the captured bacteria

1 mM SAH in 10 mM sodium phosphate buffer pH 6 was introduced into the channel containing spatially assembled *E. coli* at a flow rate of 0.11 μL min<sup>-1</sup> for 16 hours. To estimate the amount of AI-2 synthesized by the nanofactories at the captured cell surface, the effluent from the channel was collected and analyzed for its homocysteine concentration, a byproduct of the AI-2 synthesis reaction produced in stoichiometric amounts.<sup>11</sup> To estimate homocysteine concentration, the collected effluent was added to DTNB reagent (100 μM DTNB, 2.5 mM sodium acetate in 0.1 M Tris buffer, pH 8) for at least 15 minutes at room temperature. The  $od_{412}$  was measured and the concentration of homocysteine (equal to the AI-2 concentration) calculated using the molar extinction coefficient (13 600 M<sup>-1</sup> cm<sup>-1</sup>) of the reaction product 5-thio-2-nitrobenzoic acid (TNB).<sup>39</sup> All the above steps were performed in the control channel except for the introduction of the nanofactories.

### Manipulation of the QS response of captured bacteria within the bioMEMS device using biological nanofactories

*E. coli* W3110 carrying plasmids pCT5 and pETGFP were captured on the working electrode using the scheme described above. These cells produce their own AI-2 and carry plasmids that produce GFP in response to AI-2. In addition, AI-2 was synthesized at the surface of the captured cells *via* the nanofactories by introducing 1 mM SAH dissolved in LB medium for 84 hours at a flow rate of 0.11 μL min<sup>-1</sup>. Two controls were performed: one in which all the above steps were carried out except for the addition of the nanofactories and another in which all steps were performed except for the introduction of SAH into the microchannel (nanofactories were added here). At the end of 82 hours, the channels were rinsed with PBS. To monitor the response of the cells, the AI-2 based fluorescence (GFP expression) of the cells was observed as a function of time under the microscope and images were taken using the digital camera.

## Results and discussion

### Spatially selective assembly of the biological nanofactories

When HGLPT and tyrosinase are mixed in solution, tyrosinase activates the tyrosine residues of the C-terminal pentatyrosine tag of HGLPT generating reactive *o*-quinones. Upon introduction into the channel, the *o*-quinones react with the amine groups of chitosan on the working electrode thereby conjugating HGLPT to chitosan.<sup>26–29</sup> This comprises a second assembly domain for the nanofactory; in this case it demonstrates the assembly of the nanofactory onto a specific electronically signaled area. When Alexa Fluor 568 labeled anti-*E. coli* is subsequently added to the microchannel, the protein G component of HGLPT binds to the Fc region of the introduced antibody causing the antibody to be attached to the working electrode (*via* HGLPT and chitosan). Fig. 2a shows the scheme for the spatially selective attachment of the nanofactories.

Fig. 2b shows photographs of the working electrodes (with electrodeposited chitosan) and reference electrodes (without electrodeposited chitosan but within the same channel) in both the experimental (with tyrosinase, HGLPT and antibodies) and control channels (HGLPT and antibodies; no tyrosinase). Fig. 2c shows that the average fluorescence (grayscale intensity, in arbitrary units) observed for the working electrode in the experimental channel is  $\sim 122$  while that observed for the experimental reference electrode is  $\sim 11$ , *i.e.* an order of magnitude lower. In the control channel, the observed fluorescence

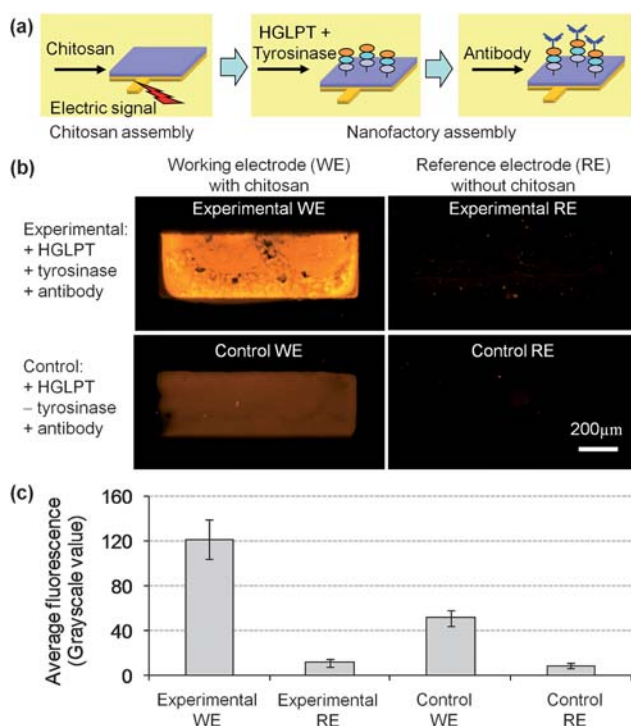


**Fig. 2** Spatially selective assembly of biological nanofactories within the device. (a) Experimental process. (b) Photographs of the working (with chitosan) and reference electrodes (without chitosan) in the experimental (containing HGLPT, tyrosinase and antibodies) and control (containing HGLPT and antibodies) channels after fluorescent nanofactory assembly. (c) Fluorescence observed for the working and reference electrodes of both channels.

intensities for the working and reference electrodes are  $\sim 52$  and  $\sim 8$ . Comparing the working electrodes in both channels, the fluorescence in the experimental channel is 2.3 times that observed in the control channel. The relatively high non-specific binding may be associated with chitosan non-specifically binding both the HGLPT and the antibody, which would be consistent with literature reports where chitosan is commonly used as a coagulant.<sup>28,40</sup> The non-uniformity of the fluorescence on the experimental working electrode is in part due to defects on the electrode surface. Delamination in the bottom left-most corners (Fig. 2b) might be a result of fluid shear stress as the flow was from left to right in the images.

Overall, results depicted in Fig. 2 support the conclusion that our conceived assembly scheme worked. That is, electrodeposited chitosan serves as an attachment interface for spatially selective and covalent assembly of nanofactories in the microchannel.

### Spatially selective capture of bacteria and *in vitro* synthesis of AI-2 at the surface of the captured bacteria

We next demonstrate the capture of bacteria (*E. coli* BL21 pGFP overexpressing GFP) by the biological nanofactories (Fig. 3a). Fig. 3b shows that when the average observed fluorescence (grayscale intensity) for the experimental working electrode (+ nanofactories + *E. coli*) is  $\sim 3$  times that observed for the control working electrode (– nanofactories + *E. coli*). Chitosan is capable of capturing bacteria in both experimental and control microchannels (due to non-specific binding).<sup>27,41,42</sup> Therefore the increase observed for the experimental working electrode over the control working electrode indicates the contribution of the nanofactories in the cell capture. Fig. 3b demonstrates that the nanofactories are capable of capturing bacteria in a spatially selective manner. Because the antibodies are fixed to the Pfs–LuxS–protein G chimeric enzyme, when substrate S-ribosylhomocysteine (SAH) is introduced into the channel, it is “sensed” by Pfs and converted into product SRH. In this way, Pfs and LuxS in the nanofactory together enzymatically convert SAH to AI-2. Fig. 3c shows the AI-2 concentrations measured in the outflows from the experimental and control channels. The AI-2 concentration in the experimental channel was  $17.1 \mu\text{M}$  while that in the control channel was  $4.6 \mu\text{M}$  (the flow rate in these experiments was  $0.11 \mu\text{L min}^{-1}$ ). The non-zero value observed in the control channel can be attributed to the low sensitivity of the AI-2 detection assay as well as trace thiols present in the channel outflow. Due to reflected fluorescence from the SU-8 microchannel sidewalls (from intrinsic SU-8 fluorescence and any non-specifically deposited bacteria), the sidewalls are not shown in Fig. 3b. The small rectangular bright spot in the control channel is likely due to a non-uniformity in the deposited chitosan. Overall, Fig. 3 demonstrates that the assembled biological nanofactories are capable of effectively capturing cells as well as synthesizing AI-2 at the surface of the captured cells.

### Elicitation of the QS response of captured bacteria within the bioMEMS device using biological nanofactories

Finally, we demonstrate the manipulation of quorum sensing (QS) bacteria by *in situ* small molecule synthesis. *E. coli* W3110

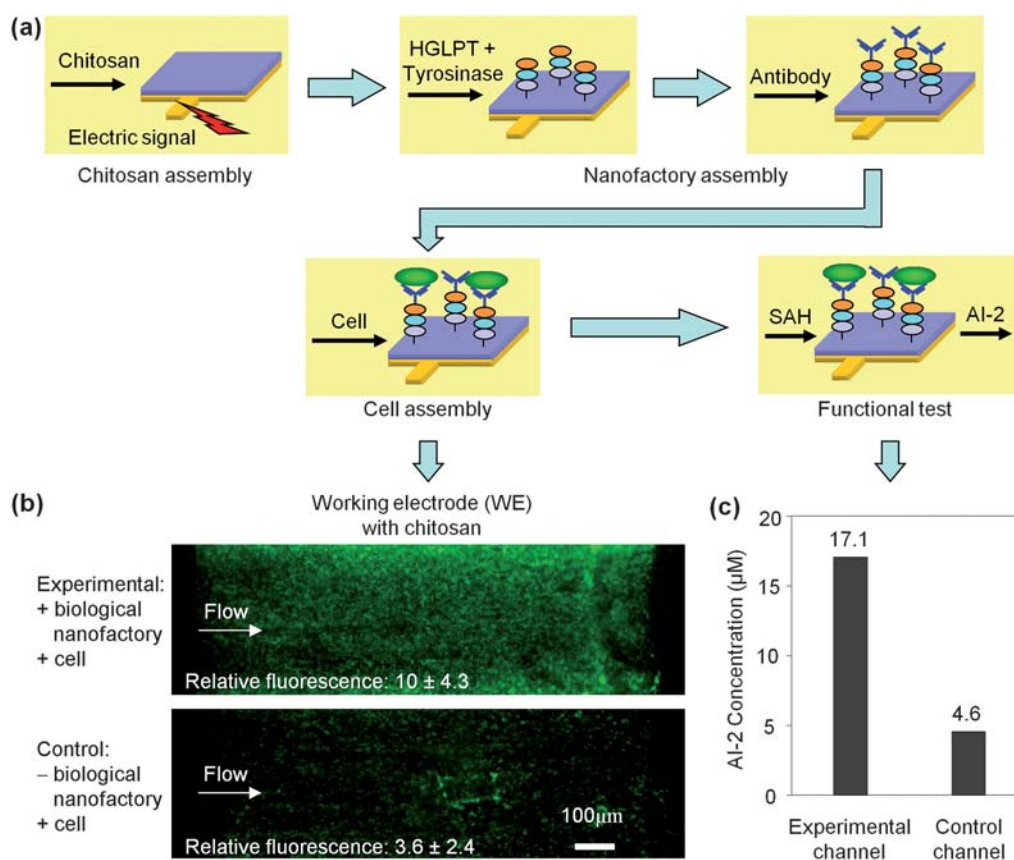


**Fig. 3** Testing the functioning (bacterial capture and AI-2 synthesis capabilities) of the spatially assembled nanofactories. (a) Experimental process for cell assembly and activity testing. (b) Photographs of the working electrodes in the experimental channel (containing nanofactories) and in the control channel (without nanofactories). The indicated fluorescence intensity is shown relative to that observed for the experimental working electrode (which is set to 10). (c) AI-2 concentrations synthesized by nanofactories in the experimental and control channels (measured in the channel outflows).

carrying plasmids pCT5 and pETGFP are spatially captured on the working electrode *via* the biological nanofactories. These plasmids were specifically constructed to enable GFP expression in direct response to AI-2 signaling.<sup>37</sup> When SAH is introduced into the channel, the biological nanofactories synthesize AI-2. The bacteria sense the local AI-2 and trigger their QS response, *i.e.* produce AI-2 dependent GFP (Fig. 4a). In addition to AI-2 produced by the nanofactories, *E. coli* W3110 produces its own AI-2, which contributes to the overall GFP expression. To quantify the contribution of the native AI-2 on the QS response (GFP expression), controls were performed where *E. coli* W3110 (containing both plasmids) were separately captured with either electrodeposited chitosan (– nanofactories) or by the biological nanofactories (– SAH introduction).

Fig. 4b shows the AI-2 dependent GFP expression (relative fluorescence) observed for the working electrodes of the experimental and control channels during 82 hours in LB medium. The GFP level in the control channels initially increases ( $\sim 20$  hours) and subsequently begins to decrease. In the experimental channel, the GFP level is significantly higher than that observed in the control channels at all times (up to 82 hours), and a similar profile (slow increase and slow decrease) was found. Fig. 4c and d show photographs and the relative fluorescence of the working electrodes of the experimental and control channels after the final PBS rinse. The relative fluorescence in the experimental channel

is  $\sim 3$  times greater than that observed in both control channels. It is interesting that this enhancement is comparable to that observed in Fig. 3c for downstream measurement of AI-2 production. Because these cells produce their own AI-2 and carry plasmids that produce GFP in response to AI-2, lower fluorescence (compared to the experimental channel) is observed in both controls after final PBS rinse. The higher fluorescence abnormality observed for the right hand side of the control\_2 WE electrode is probably due to the formation of an uneven chitosan hydrogel formed during electrodeposition.

An explanation for the observed trends is that in the control channels, the cells which had been captured for the previous  $\sim 1.5$  hours (cell introduction and rinsing steps) are in a slowly metabolized state and produce AI-2 and GFP at slower rates than otherwise would be expected in shake flask batch cultures.<sup>43</sup> The control channels which contain AI-2 producing cells exhibit similar initial rates of GFP synthesis but at reduced levels due to the absence of AI-2-synthesizing nanofactories. The apparent decay in GFP may be due to the sloughing of proliferating cells after initial attachment and the native QS response. That is, in the experimental case, AI-2 is known to stimulate biofilm formation;<sup>44</sup> the longevity and magnitude of the fluorescence support a conclusion that there was enhanced biofilm formation and some of these cells could have sloughed off over time.

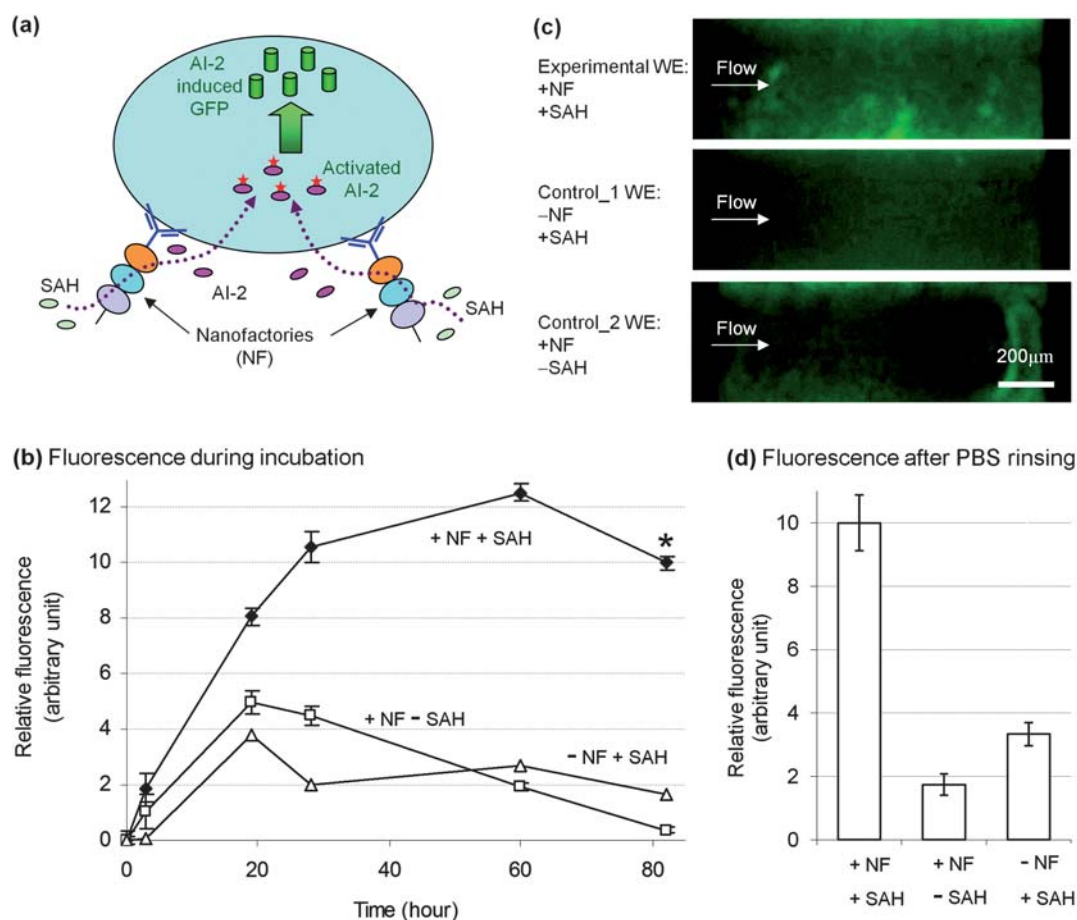


**Fig. 4** Manipulation of the QS response of bacteria in the bioMEMS device using biological nanofactories. (a) AI-2 synthesized locally and delivered at the surface of the captured bacteria by the biological nanofactories triggers a manipulated AI-2 dependent QS response (GFP production). (b) Progression of the QS response (GFP production; relative fluorescence) in the experimental and control channels monitored over three days (82 hours). Photographs (c) and relative fluorescence (d) of the working electrodes in the experimental and control channels after 82 hours of AI-2 induced GFP expression and PBS rinsing (where fluorescence intensity is normalized to 10 at the 82 hour data point (\*)).

## Conclusions

In this work, we presented biological nanofactories as a technique for the spatially selective capture and manipulation of the QS response of bacteria within a bioMEMS device. The biological nanofactories comprising of targeting (antibody), sensing (Pfs), synthesis (Pfs and LuxS) and assembly modules (both the protein G and the pentatyrosine tag) were shown to be assembled in a spatially selective manner onto the electrodeposited chitosan scaffold within the device (Fig. 2). The assembled nanofactories were capable of capturing targeted QS bacteria and synthesizing AI-2 from SAH (Fig. 3). Finally the nanofactories were demonstrated to alter the native progression of the QS response of captured cells within the device (GFP expression, Fig. 4).

Our technique provides a platform for interrogating the interaction of bacteria and small signaling molecules in a spatially selective manner within controlled microenvironments. Specifically, the QS response of bacteria (biofilm formation, reporter production) can be observed as a function of controllable parameters such as flow rate, temperature, pH, *etc.* While the effect of AI-2 on the QS response of bacteria such as *E. coli* and *Salmonella typhimurium* has been described,<sup>43,45,46</sup> it

remains to be investigated in other AI-2 responsive bacteria. We envision our technique being used as a test-bed for investigating the cell-cell communication as a means for developing new antimicrobials based on QS modulation.

## Acknowledgements

This work was supported in part by the Robert W. Deutsch Foundation, the Defense Threat Reduction Agency (DTRA), and the NSF-EFRI program (#0735987). We acknowledge facilities provided by the Maryland NanoCenter and its FabLab. We are also thankful for helpful discussions within the Rubloff and Bentley research teams and with the Biochip Collaborative ([www.biochip.umd.edu](http://www.biochip.umd.edu)) at University of Maryland.

## References

- 1 A. Camilli and B. L. Bassler, *Science*, 2006, **311**, 1113–1116.
- 2 U. Jenal and C. J. Dorman, *Curr. Opin. Microbiol.*, 2009, **12**, 125–128.
- 3 D. W. Wolan, J. A. Zorn, D. C. Gray and J. A. Wells, *Science*, 2009, **326**, 853–858.
- 4 X. Chen, S. Schauder, N. Potier, A. Van Dorselaer, I. Pelczar, B. L. Bassler and F. M. Hughson, *Nature*, 2002, **415**, 545–549.

- 5 C. M. Waters and B. L. Bassler, *Genes Dev.*, 2006, **20**, 2754–2767.
- 6 D. A. Higgins, M. E. Pomianek, C. M. Kraml, R. K. Taylor, M. F. Semmelhack and B. L. Bassler, *Nature*, 2007, **450**, 883–886.
- 7 R. Le Berre, S. Nguyen, E. Nowak, E. Kipnis, M. Pierre, F. Ader, R. Courcol, B. P. Guery and K. Faure, *Clin. Microbiol. Infect.*, 2008, **14**, 337–343.
- 8 K. R. Hardie and K. Heurlier, *Nat. Rev. Microbiol.*, 2008, **6**, 635–643.
- 9 Y. Irie and M. R. Parsek, *Curr. Top. Microbiol. Immunol.*, 2008, **322**, 67–84.
- 10 W. C. Fuqua, S. C. Winans and E. P. Greenberg, *J. Bacteriol.*, 1994, **176**, 269–275.
- 11 C. A. Lowery, T. J. Dickerson and K. D. Janda, *Chem. Soc. Rev.*, 2008, **37**, 1337–1346.
- 12 D. T. Hung, E. A. Shakhnovich, E. Pierson and J. J. Mekalanos, *Science*, 2005, **310**, 670–674.
- 13 D. A. Rasko, C. G. Moreira, R. Li de, N. C. Reading, J. M. Ritchie, M. K. Waldor, N. Williams, R. Taussig, S. Wei, M. Roth, D. T. Hughes, J. F. Huntley, M. W. Fina, J. R. Falck and V. Sperandio, *Science*, 2008, **321**, 1078–1080.
- 14 A. Vendeville, K. Winzer, K. Heurlier, C. M. Tang and K. R. Hardie, *Nat. Rev. Microbiol.*, 2005, **3**, 383–396.
- 15 D. J. Beebe, G. A. Mensing and G. M. Walker, *Annu. Rev. Biomed. Eng.*, 2002, **4**, 261–286.
- 16 J. W. Hong and S. R. Quake, *Nat. Biotechnol.*, 2003, **21**, 1179–1183.
- 17 J. W. Hong, V. Studer, G. Hang, W. F. Anderson and S. R. Quake, *Nat. Biotechnol.*, 2004, **22**, 435–439.
- 18 E. A. Ottesen, J. W. Hong, S. R. Quake and J. R. Leadbetter, *Science*, 2006, **314**, 1464–1467.
- 19 J. Atencia and D. J. Beebe, *Nature*, 2005, **437**, 648–655.
- 20 U. Bilitewski, M. Genrich, S. Kadow and G. Mersal, *Anal. Bioanal. Chem.*, 2003, **377**, 556–569.
- 21 J. Shim, T. F. Bersano-Begey, X. Y. Zhu, A. H. Tkaczyk, J. J. Linderman and S. Takayama, *Curr. Top. Med. Chem.*, 2003, **3**, 687–703.
- 22 R. Fernandes, V. Roy, H. C. Wu and W. E. Bentley, *Nat. Nanotechnol.*, 2010, DOI: 10.1038/nnano.2009.457.
- 23 P. R. Leduc, M. S. Wong, P. M. Ferreira, R. E. Groff, K. Haslinger, M. P. Koonce, W. Y. Lee, J. C. Love, J. A. McCammon, N. A. Monteiro-Riviere, V. M. Rotello, G. W. Rubloff, R. Westervelt and M. Yoda, *Nat. Nanotechnol.*, 2007, **2**, 3–7.
- 24 L. Bjorck and G. Kronvall, *J. Immunol.*, 1984, **133**, 969–974.
- 25 U. Sjobring, L. Bjorck and W. Kastern, *J. Biol. Chem.*, 1991, **266**, 399–405.
- 26 T. H. Chen, D. A. Small, L. Q. Wu, G. W. Rubloff, R. Ghodssi, R. Vazquez-Duhalt, W. E. Bentley and G. F. Payne, *Langmuir*, 2003, **19**, 9382–9386.
- 27 R. Fernandes, C. Y. Tsao, Y. Hashimoto, L. Wang, T. K. Wood, G. F. Payne and W. E. Bentley, *Metab. Eng.*, 2007, **9**, 228–239.
- 28 A. T. Lewandowski, D. A. Small, T. H. Chen, G. F. Payne and W. E. Bentley, *Biotechnol. Bioeng.*, 2006, **93**, 1207–1215.
- 29 X. L. Luo, A. T. Lewandowski, H. M. Yi, G. F. Payne, R. Ghodssi, W. E. Bentley and G. W. Rubloff, *Lab Chip*, 2008, **8**, 420–430.
- 30 J. Vinsova and E. Vavrikova, *Curr. Pharm. Des.*, 2008, **14**, 1311–1326.
- 31 V. K. Mourya and N. N. Inamdar, *React. Funct. Polym.*, 2008, **68**, 1013–1051.
- 32 R. Fernandes, L. Q. Wu, T. H. Chen, H. M. Yi, G. W. Rubloff, R. Ghodssi, W. E. Bentley and G. F. Payne, *Langmuir*, 2003, **19**, 4058–4062.
- 33 L. Q. Wu, H. M. Yi, S. Li, G. W. Rubloff, W. E. Bentley, R. Ghodssi and G. F. Payne, *Langmuir*, 2003, **19**, 519–524.
- 34 L. Q. Wu, A. P. Gadre, H. M. Yi, M. J. Kastantin, G. W. Rubloff, W. E. Bentley, G. F. Payne and R. Ghodssi, *Langmuir*, 2002, **18**, 8620–8625.
- 35 J. J. Park, X. L. Luo, H. M. Yi, T. M. Valentine, G. F. Payne, W. E. Bentley, R. Ghodssi and G. W. Rubloff, *Lab Chip*, 2006, **6**, 1315–1321.
- 36 C. F. Wu, H. J. Cha, G. Rao, J. J. Valdes and W. E. Bentley, *Appl. Microbiol. Biotechnol.*, 2000, **54**, 78–83.
- 37 X. W. Shi, C. Y. Tsao, X. Yang, Y. Liu, P. Dykstra, G. W. Rubloff, R. Ghodssi, W. E. Bentley and G. F. Payne, *Adv. Funct. Mater.*, 2009, **19**, 2072–2080.
- 38 X. Luo, D. L. Berlin, S. Buckhout-White, W. E. Bentley, G. F. Payne, R. Ghodssi and G. W. Rubloff, *Biomed. Microdevices*, 2008, **10**, 899–908.
- 39 J. Janatova, J. K. Fuller and M. J. Hunter, *J. Biol. Chem.*, 1968, **243**, 3612–3622.
- 40 W. G. Malette, H. J. Quigley, R. D. Gaines, N. D. Johnson and W. G. Rainer, *Ann. Thorac. Surg.*, 1983, **36**, 55–58.
- 41 H. Honda, A. Kawabe, A. Shinkai and T. Kobayashi, *J. Ferment. Bioeng.*, 1998, **86**, 191–196.
- 42 H. Honda, A. Kawabe, M. Skinkai and T. Kobayashi, *Biochem. Eng. J.*, 1999, **3**, 157–160.
- 43 L. Wang, Y. Hashimoto, C. Y. Tsao, J. J. Valdes and W. E. Bentley, *J. Bacteriol.*, 2005, **187**, 2066–2076.
- 44 A. F. G. Barrios, R. J. Zuo, Y. Hashimoto, L. Yang, W. E. Bentley and T. K. Wood, *J. Bacteriol.*, 2006, **188**, 305–316.
- 45 M. E. Taga, S. T. Miller and B. L. Bassler, *Mol. Microbiol.*, 2003, **50**, 1411–1427.
- 46 K. B. Xavier and B. L. Bassler, *J. Bacteriol.*, 2005, **187**, 238–248.